SUPPLEMENTAL MATERIAL

Ventricular myocyte cell model

The base cell model used was the human ventricular myocyte model by O'Hara et al [1] with the endocardial control parameters. To address a well-known tissue propagation issue, the I_{Na} m-gate steady-state activation curve was left-shifted by 10 mV. To simulate the different congenital LQTS subtypes, the conductance of I_{Ks} or I_{Kr} was completely blocked in the case of LQT1 and LQT2 respectively, and the conductance of I_{NaL} was increased in LQT3. To simulate the bulk heterogeneity, the conductances of I_{Kr} in LQT1, I_{Ks} in LQT2, and I_{NaL} in LQT3 were adjusted to create a repolarization gradient. The $I_{Ca,L}$ steady-state activation and inactivation curves were taken from either the original O'Hara et al formulation or another human measurement from Li et al [2], parameterized in the form of $d_\infty = 1/(1 + \exp\left[\frac{-(V+d_{\infty,V})}{d_{\infty,k}}\right])$ and $f_\infty = 1/(1 + \exp\left[\frac{V+f_{\infty,V}}{f_{\infty,k}}\right])$.

The parameters for LQT1 were: G_{Ks} = 0 mS/µF, $G_{Kr,1}$ = 0.025 mS/µF, $G_{Kr,2}$ = 0.017 mS/µF, $d_{\infty,V}$ = 3.940 mV, $d_{\infty,k}$ = 4.230 mV, $f_{\infty,V}$ = 19.58 mV, $f_{\infty,k}$ = 3.696 mV.

The parameters for LQT2 were: G_{Kr} = 0 mS/µF, $G_{Ks,1}$ = 0.050 mS/µF, $G_{Ks,2}$ = 0.030 mS/µF, $d_{\infty,V}$ = 4.8 mV, $d_{\infty,k}$ = 6.2 mV, $f_{\infty,V}$ = 28.5 mV, $f_{\infty,k}$ = 7.8 mV.

The parameters for LQT3 were: $G_{NaL,1}$ = 0.050 mS/µF, $G_{NaL,2}$ = 0.066 mS/µF, $d_{\infty,V}$ = 4.8 mV, $d_{\infty,k}$ = 6.2 mV, $f_{\infty,V}$ = 28.5 mV, $f_{\infty,k}$ = 7.8 mV.

Anatomical ventricle modeling

The anatomical geometry of the ventricle model and fiber direction field were obtained from previous work by Ten Tusscher et al [3], consisting of ~1.7 million voxels of 0.5 mm size, incorporating a Purkinje network (Fig.S1).

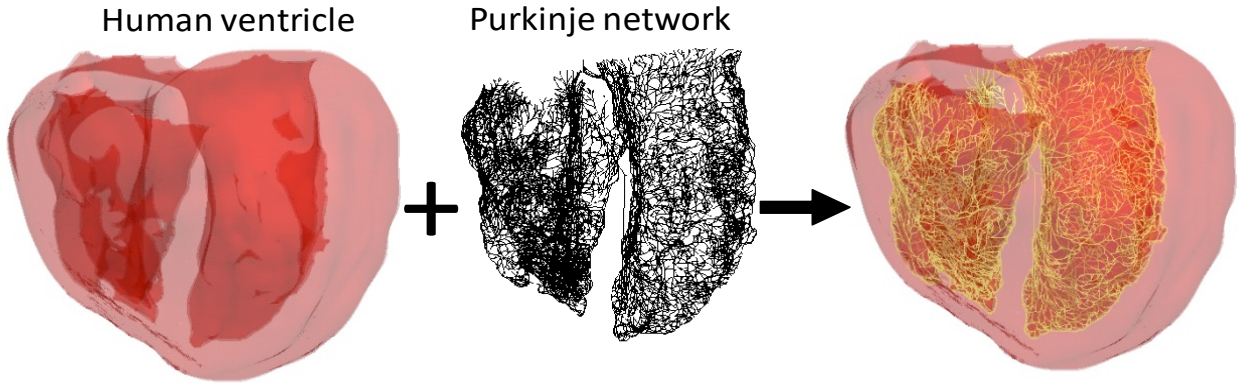

Figure S1. Human ventricle myocardium model coupled with the Purkinje network model. The Purkinje network starts at the simulated AV node where sinus beats are initiated, is grown onto the endocardial surface.

The partial differential equation governing membrane voltage V in the anatomical model is:

$$\frac{\partial V}{\partial t} = -I_{ion}/C_m + \sum_i \sum_j \frac{\partial}{\partial x_i} D_{ij} \frac{\partial}{\partial x_j} V$$

where C_m = 1 μF/cm^2 is the membrane capacitance, I_{ion} is the total ionic currents of the cell, and D_{ij} is the 3D conductivity tensor describing the anisotropy of voltage propagation corresponding to the fiber direction field, with i,j as indices for the 3 cartesian dimensions. Numerical integration was performed using with a finite difference forward Euler method and an operating splitting and time adaptive algorithm [4] with the time step (Δt) varying between 0.01 ms and 0.1 ms. A bulk heterogeneity in the RV was set using the parameters described above (Fig.S2).

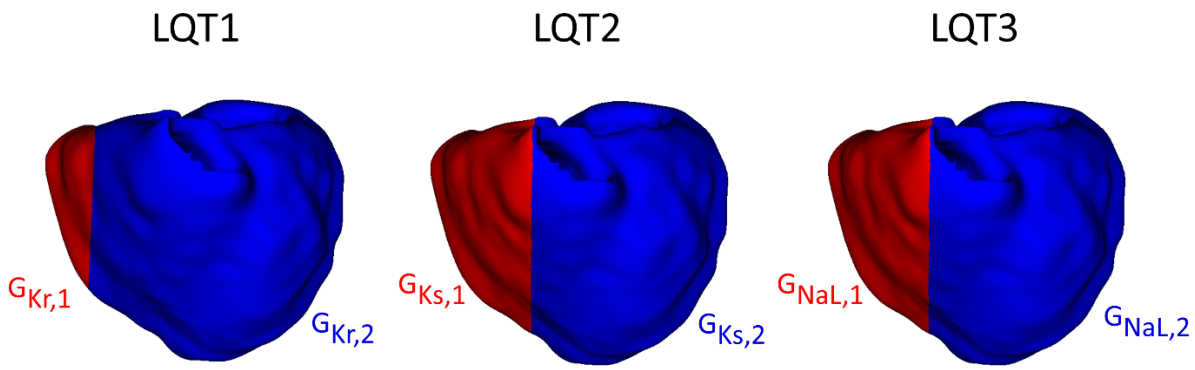

Figure S2. Bulk heterogeneities for each LQTS subtype. The spatial heterogeneity is created using two different conductance regions in G_{Kr} for LQT1, G_{Ks} for LQT2, and G_{NaL} for LQT3. All other parameters are homogeneous across the ventricle for each subtype. The smaller $G_{Kr,1}$ region used in LQT1 was to avoid 2:1 block when demonstrating arrhythmogenesis at fast pacing.

Purkinje network modeling

We tailored our model to provide for a physiological activation sequence, ECG properties, and robust forward and retrograde conduction at the Purkinje-myocyte junctions (PMJs). The human Purkinje action potential model by Stewart et al [5] was used for our Purkinje network. The Purkinje network was modeled as a connected set of 1D cables with the diffusion constant set to result in a conduction velocity of ~4 m/s. The primary tree of the Purkinje network began at a straight His-bundle which then branched into the right bundle branch and the left bundle branch (including the left anterior and posterior fascicles). An AV-node delay was simulated by a very slow diffusion constant at the beginning of the His-bundle. The rest of the network was generated using a fractal surface mapping method developed by Sahli Costabal et al [6], mapped to the RV and LV endocardial surfaces. The terminal Purkinje fibers were allowed to form loops as

consistent with experimental data [7, 8]. The final full structure (Fig.S1) consisted of 58,705 computational cell nodes with Δx = 0.5 mm. A PMJ was created between each Purkinje cell node to the closest ventricular myocyte cell node, modeled as a passive Ohm's law conductance. The relative capacitance ratio between the Purkinje and ventricular myocyte computational nodes was set to 1.0 which allowed for robust forward and retrograde conduction across the PMJ.

The differential equation governing Purkinje cell voltage V_P is:

$$\frac{dV_P}{dt} = -\frac{I_{ion,P}}{C_{m,P}} + \sum_i D_P \frac{V_i - V_p}{\Delta x^2} + I_{PMJ}/C_{m,P}$$

with

$$I_{PMJ} = \begin{cases} G_{PMJ}(V - V_P), & \text{cells with a PMJ} \\ 0, & \text{cells without a PMJ} \end{cases}$$

where $C_{m,Purkinje}$ is the capacitance of the Purkinje cell node, $I_{ion,Purkinje}$ is the total ionic currents of the Purkinje cell, $D_{Purkinje}$ = 0.0300 cm^2/ms is the diffusion constant, G_{PMJ} = 0.05 mS/μF. The ventricular myocyte that belongs to the PMJ also receives an equal and opposite I_{PMJ}. Numerical integration was performed using a finite difference forward Euler method with operator splitting and a fixed time step of Δt = 0.01 ms.

1D and 2D tissue models

The partial differential equation governing voltage for the 1D cable is

$$\frac{\partial V}{\partial t} = -I_{ion}/C_m + D\frac{\partial^2 V}{\partial x^2}$$

where V is the membrane voltage, C_m=1 μF/cm^2 is the membrane capacitance, D = 0.0005 cm^2/ms is the diffusion constant (proportional to gap junction conductance), and Δx = 0.15 mm.

For 2D tissue, the equation for voltage is

$$\frac{\partial V}{\partial t} = -I_{ion}/C_m + D(\frac{\partial^2 V}{\partial x^2} + \frac{\partial^2 V}{\partial y^2})$$

where V is the membrane voltage, C_m=1 μF/cm^2 is the membrane capacitance, D = 0.0001 cm^2/ms is the diffusion constant (proportional to gap junction conductance), and Δx = 0.15 mm.

Numerical integration was performed using a finite difference forward Euler method and an operating splitting and time adaptive algorithm with the time step (Δt) varying between 0.01 ms and 0.1 ms.

Pseudo-ECG computation

Pseudo ECGs were computed using the following formula [9, 10]

$$\boldsymbol{\Phi_e}(x', y', z') \sim \iiint (-\boldsymbol{\nabla} V) \cdot \left[\boldsymbol{\nabla} \frac{1}{r}\right] dxdydz$$

where $\boldsymbol{\nabla} V$ is the spatial gradient of the membrane voltage and $r = [(x - x')^2 + (y - y)^2 + (y - y')^2]^{1/2}$ represents the distance from a source point (*x,y,z*) to a field point (*x',y',z'*), with the integral performed over all heart cells.

For the human ventricle simulations, we calculated a pseudo-ECG for V1 to V6 (see Fig.S3 for lead placement). A bandpass filter of 0.1-150 Hz was applied to each recording.

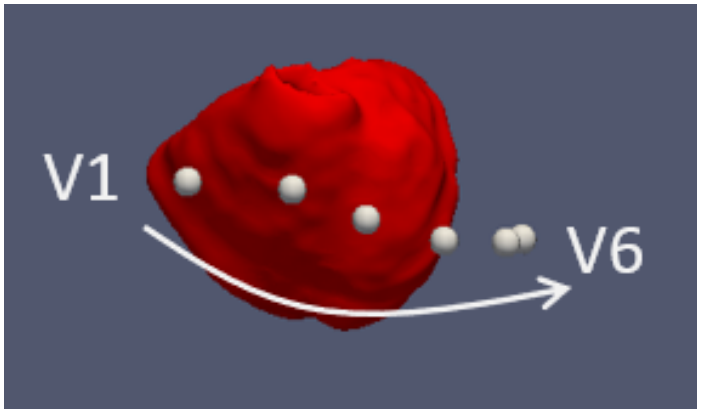

Figure S3. Lead placement for pseudo-ECG computation.

Visualization methods

Single cell, 1D, and 2D results were visualized in Python using the Matplotlib library [11]. ECGs were also plotted in Python using the Matplotlib library. Anatomical heart results were visualized in 3D using the VisIt software tool (Lawrence Livermore National Laboratory) [12].

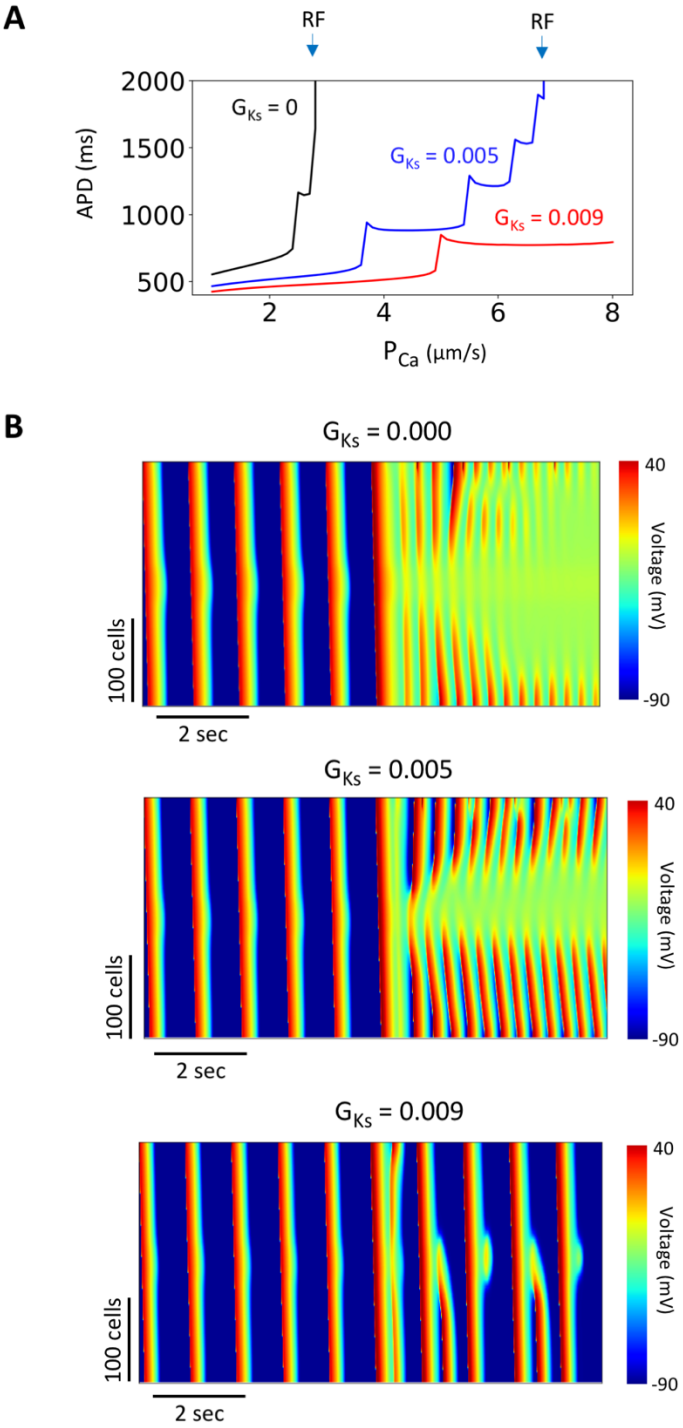

Figure S4. Effect of adding I_{Ks} back to LQT1. A) Single cell APD versus P_{Ca} for LQT1 (G_{Ks}=0 mS/μF) as in Fig.6A but with varying amounts of I_{Ks} added back. B) Linescans of voltage in a 1D cable for P_{Ca} = 4.1 μm/s at PCL=1000 ms as in Fig.6C but with varying amounts of I_{Ks} added back.

Movie Captions

Movie 1. Spontaneous initiation of arrhythmia in LQT2. Three view movie including ventricle voltage maps (left), wavefronts (colored red, middle), and Purkinje network voltage maps (right). The ECG strip and time marker are shown below. P_{Ca} ramp protocol simulation with $P_{Ca,H}$ = 2.8 μm/s (corresponding to the 6th ECG trace in Fig.2).

Movie 2. 2D simulation of spontaneous focal arrhythmias from the R-from-T mechanism. Voltage map from the 2D tissue corresponding to Fig.3D.

Movie 3. 2D simulation of spontaneous reentrant arrhythmias from the R-from-T mechanism. Voltage map from the 2D tissue corresponding to Fig.3E.

Movie 4. Spontaneous initiation of arrhythmia in LQT3. Three view movie including ventricle voltage maps (left), wavefronts (colored red, middle), and Purkinje network voltage maps (right). The ECG strip and time marker are shown below. P_{Ca} ramp protocol simulation with $P_{Ca,H}$ = 3.2 μm/s (corresponding to the 6th ECG trace in Fig.4).

Movie 5. Spontaneous initiation of arrhythmia in LQT1. Three view movie including ventricle voltage maps (left), wavefronts (colored red, middle), and Purkinje network voltage maps (right). The ECG strip and time marker are shown below. P_{Ca} ramp protocol simulation with $P_{Ca,H}$ = 3.1 μm/s at 60 bpm (corresponding to the 4th ECG trace in Fig.5).

Movie 6. Schematic diagram distinguishing the "R-to-T" and "R-from-T" mechanisms of arrhythmia initiation. Animated version of Figure 8 in the main text.

References

1. O'Hara T, Virág L, Varró A, Rudy Y. Simulation of the undiseased human cardiac ventricular action potential: model formulation and experimental validation. PLoS Comput Biol. 2011;7(5):e1002061.
2. Li GR, Yang B, Feng J, Bosch RF, Carrier M, Nattel S. Transmembrane ICa contributes to rate-dependent changes of action potentials in human ventricular myocytes. Am J Physiol. 1999;276(1 Pt 2):H98-H106.
3. Ten Tusscher KH, Mourad A, Nash MP, et al. Organization of ventricular fibrillation in the human heart: experiments and models. Exp Physiol. 2009;94(5):553-62.
4. Qu Z, Garfinkel A, An advanced algorithm for solving partial differential equation in cardiac conduction. IEEE Transactions on Biomedical Engineering, vol. 46, no. 9, pp. 1166-1168, Sept. 1999.
5. Stewart P, Aslanidi OV, Noble D, Noble PJ, Boyett MR, Zhang H. Mathematical models of the electrical action potential of Purkinje fibre cells. Philos Trans A Math Phys Eng Sci. 2009;367(1896):2225-55.
6. Sahli Costabal F, Hurtado DE, Kuhl E. Generating Purkinje networks in the human heart. J Biomech. 2016;49(12):2455-65.
7. De almeida MC, Lopes F, Fontes P, Barra F, Guimaraes R, Vilhena V. Ungulates heart model: a study of the Purkinje network using India ink injection, transparent specimens and computer tomography. Anat Sci Int. 2015;90(4):240-50.
8. Ijiri T, Ashihara T, Yamaguchi T, et al. A procedural method for modeling the purkinje fibers of the heart. J Physiol Sci. 2008;58(7):481-6.
9. Xie F, Qu Z, Yang J, Baher A, Weiss JN and Garfinkel A. A simulation study of the effects of cardiac anatomy in ventricular fibrillation. *J Clin Invest*. 2004;113:686-93.
10. Sadrieh A, Domanski L, Pitt-Francis J, Mann SA, Hodkinson EC, Ng CA, Perry MD, Taylor JA, Gavaghan D, Subbiah RN, Vandenberg JI and Hill AP. Multiscale cardiac modelling reveals the origins of notched T waves in long QT syndrome type 2. *Nature communications*. 2014;5:5069.
11. Hunter JD. Matplotlib: A 2D Graphics Environment. Computing in Science & Engineering. 2007;9(3):90-95. doi:10.1109/mcse.2007.55
12. Childs H, Brugger E, Whitlock B, et al. VisIt: An End-User Tool For Visualizing and Analyzing Very Large Data. High Performance Visualization Chapman & Hall/CRC Computational Science. 2012. doi:10.1201/b12985-21